In situ measures of methanotroph activity in upland soils: A reaction-diffusion model and field observation of water stress

Joseph C. von Fischer,[1,2] Gregory Butters,[3] Paul C. Duchateau,[4] Roger J. Thelwell,[4,5] and Richard Siller[1,6]

Received 19 March 2008; revised 12 September 2008; accepted 28 October 2008; published 24 February 2009.

[1] Laboratory assays of methanotroph activity in upland (i.e., well-drained, oxic) ecosystems alter soil physical structure and weaken inference about environmental controls of their natural behavior. To overcome these limitations, we developed a chamber-based approach to quantify methanotroph activity in situ on the basis of measures of soil diffusivity (from additions of an inert tracer gas to the chamber headspace), methane concentration change, and analysis of results with a reaction-diffusion model. The analytic solution to this model predicts that methane consumption rates are equally sensitive to changes in methanotroph activity and diffusivity, but that doubling either of these parameters leads to only a $\sqrt{2}$ increase in consumption. With a series of simulations, we generate guidelines for field deployments and show that the approach is robust to plausible departures from assumptions. We applied the approach on a dry grassland in north central Colorado. Our model closely fit measured changes in methane concentrations, indicating that we had accurately characterized the biophysical processes underlying methane uptake. Field patterns showed that, over a 7-week period, soil moisture fell from 38% to 15% water-filled pore spaces, and diffusivity doubled as the larger soil pores drained of water. However, methane uptake rates fell by ~40%, following a 90% decrease in methanotroph activity, suggesting that the decline in methanotroph activity resulted from water stress to methanotrophs. We anticipate that future application of this approach over longer timescales and on more diverse field sites has potential to provide important insights into the ecology of methanotrophs in upland soils.

Citation: von Fischer, J. C., G. Butters, P. C. Duchateau, R. J. Thelwell, and R. Siller (2009), In situ measures of methanotroph activity in upland soils: A reaction-diffusion model and field observation of water stress, *J. Geophys. Res.*, *114*, G01015, doi:10.1029/2008JG000731.

1. Introduction

[2] There is fundamental interest in understanding how soil biogeochemical processes relate to functional traits of soil microbes [*Green et al.*, 2008] and environmental controls of their activity [*Schimel*, 2001]. For many biogeochemical processes, understanding the linkage to microbes and their environmental controls is complicated by the myriad types of organisms and multiple environmental controls. In contrast, methane consumption in upland soils (i.e., well-drained, oxic) is relatively simple: methane molecules diffuse from the atmosphere into the soil, where they are consumed by methanotrophic bacteria [*King*, 1997]. Spatial and temporal variability in upland methane flux is thus driven by differences in soil diffusivity, methanotroph activity, or some combination of the two.

[3] A growing body of work has examined methanotroph community composition in upland soils. The phylogenetic and functional cohesiveness of methanotrophs has allowed application of molecular tools that, in turn, have generated considerable progress in identifying changes in methanotroph community structure across habitats where methane flux rates differ [*Roslev et al.*, 1997; *Radajewski et al.*, 2002; *Knief et al.*, 2003; *Horz et al.*, 2005]. But because both methanotroph activity and soil diffusivity can constrain methane uptake, the importance of biology for driving the observed differences remains unclear.

[4] Separation of the physical and biological controls on methane uptake has been constrained, in part, by the difficulty in measuring biological activity. Historically,

[1]Department of Biology, Colorado State University, Fort Collins, Colorado, USA.
[2]Graduate Degree Program in Ecology, Colorado State University, Fort Collins, Colorado, USA.
[3]Department of Soil and Crop Sciences, Colorado State University, Fort Collins, Colorado, USA.
[4]Department of Mathematics, Colorado State University, Fort Collins, Colorado, USA.
[5]Now at Department of Mathematics and Statistics, James Madison University, Harrisonburg, Virginia, USA.
[6]Also at Department of Biology, University of Michigan, Ann Arbor, Michigan, USA.

0148-0227/09/2008JG000731

methanotroph activity has been measured by returning soil to the laboratory, processing it by sieving, and incubating replicate subsamples for a period of hours or days [*Bender and Conrad*, 1992; *Gulledge and Schimel*, 1998a; *Dunfield and Conrad*, 2000]. The assay is labor intensive, not repeatable on the same sample, and it creates a disturbance to the soil physical and biological structure that limits inference about the natural activity [*Madsen*, 1998]. In contrast, soil gas diffusivity and methane consumption can be measured in situ using an inserted flux chamber. These small, portable chambers allow repeated measures on a study plot with minimal disturbance and relatively little labor. The limitations of flux chambers have been examined thoroughly [*Livingston and Hutchinson*, 1995; *Healy et al.*, 1996] with the cautionary observation that the chamber itself alters the gas exchange from the atmosphere to the soil. With increasing time, for example, the depletion of methane in the headspace of the chamber causes a reduction in methanotroph activity as compared to the surrounding soil that is exposed to ambient methane, and lateral methane diffusion could supplement the soil methane supply.

[5] To overcome the limitations of incubations and capitalize on the advantages of flux chambers, we have developed, examined and applied a new approach where we simultaneously quantify both soil gas diffusivity and methanotroph activity. This method for determining soil methanotroph activity is based on the principle that upland methane flux is a function of only two soil properties: gas transport and methanotroph activity [*Smith et al.*, 2003]. Because the relationship between flux and its two controls can be quantified mathematically, the model can be used to solve for the methanotroph activity from field measures of soil diffusivity and the methane flux rate.

[6] To formalize this new methodological approach, we develop and apply an analytic solution to quantify the reaction and diffusion of methane that is associated with use of methane flux chambers. We then evaluate our assumptions and quantify the implications of their violation. Finally, we illustrate the application of the technique by quantifying diffusive versus methanotrophic controls on methane consumption in the Shortgrass Steppe ecosystem.

2. Site Description

[7] We examined methane uptake on the soils of the Shortgrass Steppe Long-Term Ecological Research (SGS LTER) site in the grasslands of north central Colorado (40° 49′N; 104° 46′W). The climate is dry, with 320 mm mean annual precipitation. Trace gas fluxes have been studied extensively in this area [*Mosier et al.*, 1993; *Mosier et al.*, 1996; *Mosier et al.*, 1997; *Epstein et al.*, 1998; *Mosier et al.*, 1998; *Mosier et al.*, 2002]; reported rates of methane uptake range up to 3 mg CH_4-C m^{-2} d^{-1}. In a field trial of the technique during spring and early summer of 2007, we examined methane dynamics of a sandy loam soil classified as an Ustollic Haplargid.

3. Methods

3.1. Field and Laboratory Methods

[8] We deployed 18 flux chambers on each date, and arrayed them across the landscape to include the diversity of microclimatic and topographic diversity that defines the study area. Microclimatic differences spanned the range of cover from vegetated to partly or completely bare soils; topographically, we made measurements from the summit to the toe of a slope (~20 m elevation change over ~300 m transect). Chamber lids were round, 20 cm inside diameter, opaque PVC and vented, following *Livingston and Hutchinson* [1995]. Chamber bases were also opaque PVC, and they were inserted 8 ± 2 cm into the ground to maintain vertical gradients in gas concentrations during measurement. Bases were installed 30 to 60 min before flux measurement, and they were removed afterward. The lid and base nested tightly together in milled grooves on their mating surfaces, and the two were sealed by a rubber ring that fit snugly around the seam. The chamber headspace air was circulated by a small, battery-powered, brushless electric fan. Previous tests indicated that this fan was needed to mix the headspace gases.

[9] Chamber flux measurements lasted 15 min. Two minutes prior to the first measurement ($t = -2$), the fans were turned on, the lid was placed on the chamber base and 30 mL of a dilute inert tracer gas (sulfur hexafluoride or SF_6) was added to the chamber headspace and dispersed by syringe pumping. These initial steps usually took 30–45 s, leaving the inert tracer gas to mix in the headspace for about 1.5 min. Then 30 mL gas samples were taken at 5 min intervals (at $t = 0$, 5, 10, and 15 min) and transferred into preevacuated 15 mL vials, sealed with a butyl rubber septum (Geomicrobial Technologies, Oechelata, OK). Previous tests showed that samples stored in this way are stable for >3 months, though analysis was typically completed in <1 month. To account for any systematic change in gas concentrations during sample storage, we also put replicate gas standards (two levels of methane: 0 and 5 ppm) into vials while we were still in the field. We then analyzed the stored standards and corrected all samples for any systematic changes in gas concentrations exhibited by these stored samples.

[10] Gases were analyzed in the laboratory by gas chromatography on a Shimadzu GC14B with N_2 carrier gas. Injection of a single gas sample filled two sample loops on a 10-port injection valve. One sample loop led to an FID for determination of methane and carbon dioxide concentrations. The second sample loop led to an ECD for determination of the inert tracer gas. The FID circuit also included a methanizer for determination of carbon dioxide concentrations. Additional valves installed in the chromatographic flow paths and 1 m Porapack Q precolumns allowed us to divert the oxygen peaks away from the detectors, helping to maintain detector stability and sensitivity. We used 1/8″ stainless steel packed columns; 3 m Porapack QS columns were on the ECD circuit and 3 m Haysep D columns on the FID circuit. Oven temperature was 60°C. The instrument was calibrated for methane and carbon dioxide on the basis of three or more certified gas standards. Such standards were not available for the inert tracer gas, so we generated our own dilutions for calibration.

[11] At the end of each chamber measurement in the field, we measured volumetric water content of soils beneath each chamber (integrated over 0–10 cm depth) using a handheld TDR probe (Campbell Scientific). Because TDR estimates of water content can be influenced by salinity and other soil

properties, we calibrated the probe values using measures of bulk density (1.31 g cm^{-3}) and gravimetric water content for this site.

3.2. Model Development

[12] Our approach uses two gases to resolve the gas transport and reaction components. We add an inert tracer gas, one that is not initially present in the soil, into the headspace of a flux chamber containing ambient methane at $t = 0$, and we subsequently monitor the headspace concentration of both methane and the inert gas for 15 min. In this section, we present the mathematical expressions for the behavior of each gas, and then detail how the gas transport and biological activity are recovered from field data.

[13] We follow a widely recognized characterization of gas movement by diffusion [*Hillel*, 1982; *Rolston et al.*, 1991], resulting from gas concentration gradients in the soil and the soil's gas diffusivity (D). Advection of the soil gas phase is not considered because its effects are expected to be negligible. We also characterize the activity of methane oxidizing bacteria (μ, hereafter "methanotroph activity") as a first-order process [*King*, 1997; *Roslev et al.*, 1997; *Fenchel et al.*, 1998; *Snover and Quay*, 2000; *von Fischer and Hedin*, 2002], as is appropriate for enzymatically mediated processes when the concentration of substrate is well below the Michaelis-Menten half saturation constant (i.e., K_M) for that process [*Conrad*, 1999]. Throughout the derivations, we note the units for each parameter with respect to length (L), volume (V), mass (or moles, M) and time (T).

3.2.1. Inert Tracer Gas

[14] For a nonreactive gas, the governing equation for 1-D diffusion from a well mixed headspace into a semi-infinite, vertically homogeneous soil initially devoid of the gas is

$$a\frac{\partial C}{\partial t} = D\frac{\partial^2 C}{\partial x^2} \tag{1}$$

$$C(x,0) = 0 \tag{1a}$$

$$C(\infty,t) = 0 \tag{1b}$$

$$D\frac{\partial C(0,t)}{\partial x} = H\frac{\partial C(0,t)}{\partial t} \tag{1c}$$

where a is the air filled porosity ($L^3\ L^{-3}$) of the soil, D is the diffusion coefficient ($L^2\ T^{-1}$) of the gas in soil, C is the gas concentration ($M\ L^{-3}$), and H is the height of the chamber (L). The well mixed boundary condition (equation (1c)) states that the gas flux into the soil is equal to the gas loss from the headspace. As formulated, we assume that the cross-sectional area of the headspace is equivalent to the soil cross section. Other geometries of the chamber could be accommodated by replacing H with V/A, where V is the headspace volume and A is the soil cross-sectional area.

[15] The solution of equation (1) is well established [*Carslaw and Jaeger*, 1959]

$$C(x,t) = C_0\left[\exp\left(hx + \kappa t h^2\right) erfc\left(\frac{x}{2\sqrt{\kappa t}} + h\sqrt{\kappa t}\right)\right] \tag{2}$$

where

$$\kappa = {}^{D}/_{a} \qquad h = {}^{a}/_{H}$$

[16] For the gas concentration in the headspace, equation (2) simplifies to

$$C(0,t) = C_0\left(\exp(\mathrm{T})erfc\left(\sqrt{\mathrm{T}}\right)\right) \tag{3}$$

where

$$\mathrm{T} = \frac{aDt}{H^2}$$

[17] Equation (3) has been used by *Rolston et al.* [1991] and others in a chamber method for measurement of soil gas diffusivity. In the application of equations (1)–(3), it is customary to interpret D as the product of a tortuosity factor and the free-air diffusion coefficient of the gas at the prevailing temperature. Many forms of the tortuosity factor have been suggested [*Jury and Horton*, 2004] and usually involve a combination of soil porosity, air filled porosity, and some measure of pore connectivity/geometry. It is not necessary to calculate a tortuosity factor explicitly, however.

[18] Because gas diffusion is mass-dependent, the free-air diffusion coefficients of gases are related by their molecular weights [*Jost*, 1960] according to

$$\frac{D_A}{D_B} = \frac{\sqrt{\frac{m_{air}+m_A}{m_{air}m_A}}}{\sqrt{\frac{m_{air}+m_B}{m_{air}m_B}}} \tag{4}$$

where subscripts A and B refer to gases A, B, m is the molecular weight of the gas with the average molecular weight of air (m_{air}) being 28 g/mole. Using this equation, the effective diffusion coefficient of methane can be determined from an inert tracer gas of a different molecular weight. The molecular weights of CH_4 and SF_6 are 16 and 146 g/mole respectively.

3.2.2. Reactive Gas

[19] For a gas undergoing first-order degradation in the soil, but otherwise nonadsorbing to the solid phase and negligible solubility in the liquid phase, the governing equation for 1-D diffusion from a well mixed headspace into semi-infinite, vertically homogeneous soil is

$$a\frac{\partial C}{\partial t} = D\frac{\partial^2 C}{\partial x^2} - \mu a C(x,t) \tag{5}$$

$$C(x,0) = C_o \exp(-\beta x) \tag{5a}$$

$$C(\infty,t) = 0 \tag{5b}$$

$$D\frac{\partial C(0,t)}{\partial x} = H\frac{\partial C(0,t)}{\partial t} \tag{5c}$$

where μ is the methanotroph activity (T^{-1}), C_0 is the initial gas concentration at the soil surface and in the chamber headspace, and β is a shape factor (L^{-1}) for the initial distribution of the gas in the soil. The formulation of the initial condition (equation (5a)) follows from an analysis of the steady state behavior of equation (5). If the atmosphere is the only source of the gas of interest, the steady state ($\partial C/\partial t = 0$) solution of equation (5) for a constant ambient gas concentration at the surface of a semi-infinite soil is

$$C(x) = C_0 \exp\left[-x\sqrt{\frac{a\mu}{D}}\right] \tag{6}$$

suggesting an exponentially decreasing initial concentration distribution. When the initial concentration profile is at steady state, then $\beta = \sqrt{(a\mu/D)}$ in equation (5a).

[20] The solution to equation (5) can be derived using Laplace transforms, and to our knowledge it does not appear in the literature. The details of the derivation are somewhat tedious, so herein we only outline the solution, except that constants appearing in the final solution are defined in the solution outline. To simplify equation (5), we scale the problem by introducing $z = \eta x$ and $\tau = \lambda t$ such that

$$a\lambda\frac{\partial C}{\partial \tau} = D\eta^2\frac{\partial^2 C}{\partial z^2} - \mu a C(z,\tau) \tag{7}$$

and letting $D\eta^2 = a\mu$ and $\lambda = \mu$, the problem is reformulated as

$$\frac{\partial u}{\partial t} = \frac{\partial^2 u}{\partial z^2} - u(z,\tau) \tag{7a}$$

$$u(z,0) = \exp(-kz) \tag{7b}$$

$$\frac{\partial u(0,\tau)}{\partial z} = r\frac{\partial u(0,\tau)}{\partial \tau} \tag{7c}$$

where

$$u(z,t) = \frac{\mathrm{C}(z/\eta, \tau/\mu)}{C_0} \qquad \eta = \sqrt{\frac{a\mu}{D}}$$

$$k = \frac{\beta}{\eta} \qquad r = H\sqrt{\frac{\mu}{aD}}$$

[21] Applying the Laplace transform to equation (7) and the boundary conditions, and following considerable rearrangement, we find the solution in transform space (U)

$$U(z) = \frac{r - rk^2 - k}{2kr(\sigma_2 - \sigma_1)}\sum_{j=1}^{4}\Lambda_j\frac{\exp\left(-z\sqrt{s+1}\right)}{\sqrt{s+1}+\lambda_j} + \frac{\exp(-kz)}{s+1-k^2} \tag{8}$$

where

$$\sigma_1 = \frac{-1}{2r}\left(1+\sqrt{4r^2+1}\right) \qquad \sigma_2 = \frac{-1}{2r}\left(1-\sqrt{4r^2+1}\right)$$

$$\lambda_1 = -k \quad \lambda_2 = k \quad \lambda_3 = -\sigma_1 \quad \lambda_4 = -\sigma_2$$

$$\Lambda_1 = \frac{1}{k-\sigma_2} - \frac{1}{k-\sigma_1} \quad \Lambda_2 = \frac{1}{k+\sigma_2} - \frac{1}{k+\sigma_1}$$

$$\Lambda_3 = \frac{1}{\sigma_1+k} - \frac{1}{\sigma_1-k} \quad \Lambda_4 = \frac{1}{\sigma_2-k} - \frac{1}{\sigma_2+k}$$

[22] Using Laplace inversion formulas available in standard texts, the final result describing gas concentrations in time and space is

$$C(x,t) = C_0\exp\left[\mu t k^2 - k\eta x - \mu t\right] + C_0\exp(-\mu t)\left(\frac{r - rk^2 - k}{2kr(\sigma_2-\sigma_1)}\right)\sum_{j=1}^{4}\Lambda_j S(\eta x, \mu t, \lambda_j) \tag{9}$$

where

$$S(\eta x, \mu t, \lambda_j) = \left[\sqrt{\frac{1}{\pi\mu t}}\exp\left[\frac{-(\eta x)^2}{4\mu t}\right] - \lambda_j\exp\left[\eta x\lambda_j + \mu t\lambda_j^2\right]erfc\left(\frac{\eta x}{2\sqrt{\mu t}} + \lambda_j\sqrt{\mu t}\right)\right]$$

[23] For the gas concentration versus time in the chamber headspace, the solution is only marginally less complex

$$C(0,t) = C_0\exp\left[-\mu t\left(1-k^2\right)\right] + C_0\exp(-\mu t)\left(\frac{r - rk^2 - k}{2kr(\sigma_2-\sigma_1)}\right)\sum_{j=1}^{4}\Lambda_j S(0, \mu t, \lambda_j) \tag{10}$$

where

$$S(0,t,\lambda_j) = \left[\sqrt{\frac{1}{\pi\mu t}} - \lambda_j\exp\left[\mu t\lambda_j^2\right]erfc\left(\lambda_j\sqrt{\mu t}\right)\right]$$

[24] Of interest is the methane flux, q, into the soil from the chamber headspace, $D\partial C(x, t)/\partial x|_{x=0}$, which follows from equation (10) as

$$q(0,t) = \left[\eta D C_0\exp(-\mu t)\left(\frac{r - rk^2 - k}{2kr(\sigma_2-\sigma_1)}\right)\sum_{j=1}^{4}\Lambda_j\left(\frac{\partial S(0,\mu t,\lambda_j)}{\partial x}\right)\right] - k\eta D C_o\exp\left[-\mu t\left(1-k^2\right)\right] \tag{11}$$

where

$$\frac{\partial S(0,t,\lambda_j)}{\partial x} = \lambda_j\left[\sqrt{\frac{1}{\pi\mu t}} - \lambda_j\exp\left[\mu t\lambda_j^2\right]erfc\left(\lambda_j\sqrt{\mu t}\right)\right]$$

3.2.3. Determining Parameters μ and D From Field Data

[25] To recover the diffusion (D) and methanotroph activity (μ) parameters from the chamber concentration measurements we use a two-step approach, first determining D, then μ. We determine D by fitting equation (3) to the observed trends in inert tracer gas concentrations. Having measured all variables in equation (3) except the soil diffusivity, we used the Solver package in Microsoft Excel

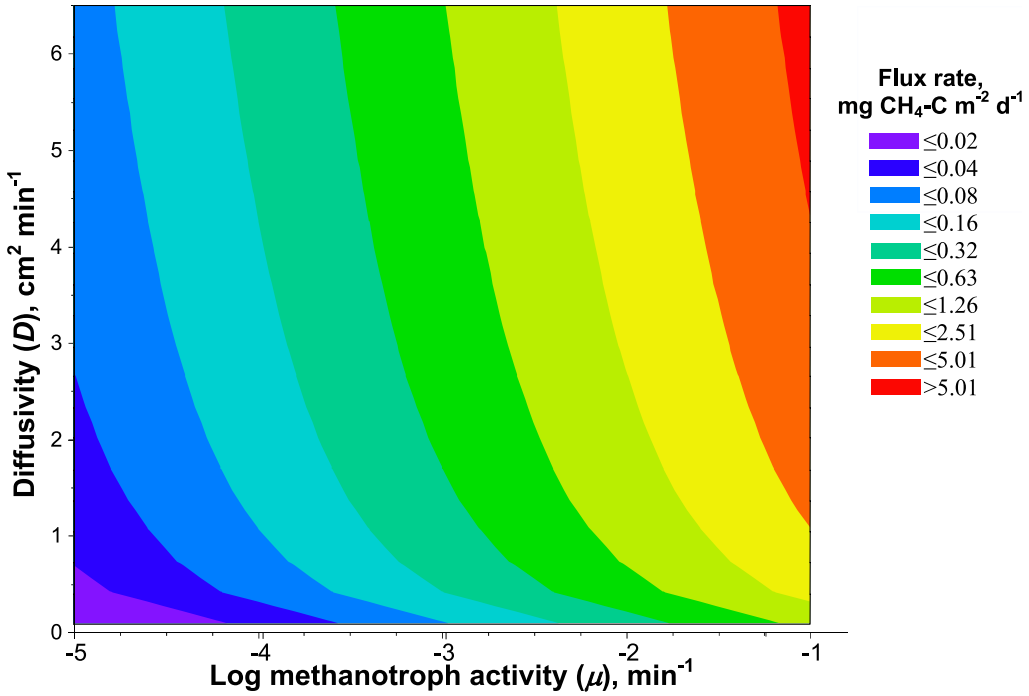

Figure 1. Effects of changing methanotroph activity (μ) and diffusivity (D) on rates of methane uptake, evaluated using equation (12) at air-filled porosity (a) of 0.35. The flux rates are reported in mg CH_4-C m^{-2} d^{-1}; note the log scale for flux units.

to iteratively find the diffusivity value that gave the smallest sum of squared error between observed and modeled (equation (3)) concentrations. With the tracer gas D so determined, the methane D is calculated directly from equation (4). To determine μ, we again used Excel's Solver to find the value of μ that minimized the difference between observed and model (equation (10)) methane concentrations. We note that current versions of Excel (i.e., Excel 2003 and 2007) include a software bug that returns an error when trying to evaluate the error function (i.e., "erf") of negative values. Users can overcome this bug either by using the identity that $\mathrm{erf}(-n) = -\mathrm{erf}(n)$ or by using a Taylor series approximation for the error function.

[26] In parallel with our iterative approach, we also developed statistical algorithms to determine D and μ from field data so that the parameters D and μ could be determined in live spreadsheets. We found a linear relationship between the inert tracer gas concentration (normalized to the initial concentration) and $\sqrt{t}$ such that the slope of this relationship was the product of $\sqrt{D}$ and another parameter, Z. This Z parameter was, in turn, a nonlinear function of H^2/a. Similarly, we found that the parameter μ was well-predicted by two terms: (1) an estimate of μ, determined by rearranging equation (12) and solving for μ; and (2) the term $\sqrt{(Da)}/H$. In comparison, we found that the iterative and statistical algorithms gave equivalent parameter estimates.

[27] Sometimes we observed field diffusivity values that were larger than physically possible. While the mechanism underlying these observations remains under continued investigation, some possible explanations include cracking of the dry soil during chamber installation, leakage from the gas flux chamber or erroneous gas concentration measures. We excluded all data from chambers with diffusivity values >6 cm^2 min^{-1}.

3.2.4. Applying D and μ to Calculate Flux From Unconfined Systems

[28] Although equation (11) might be used to estimate methane flux at any time after chamber insertion, we are actually interested in estimating methane flux at the soil surface without the confining influence of the chamber headspace. The D and μ should be used to estimate the methane flux from the ambient atmosphere using the governing equation for methane movement and uptake (equation (5)), but evaluated when the headspace imposes no restrictions on soil methane concentrations (i.e., $H \rightarrow \infty$). This unconfined, constant concentration (C_0) boundary condition in equation (5) leads to a very simple flux estimate at the soil surface

$$q(x=0) = C_0\sqrt{Da\mu} \tag{12}$$

which we will use to report methane flux for ambient conditions.

4. Results

4.1. Model Insights into Methane Biogeochemistry

[29] We evaluated equation (12) across a range of D and μ values to illustrate how variation in these parameters affects methane flux rates (Figure 1). The range of possible diffusivity values is bounded on the upper end by the free-air diffusivity of methane (~12 cm^2 min^{-1}), and on the lower end when soil pores fill up with water and diffusivity

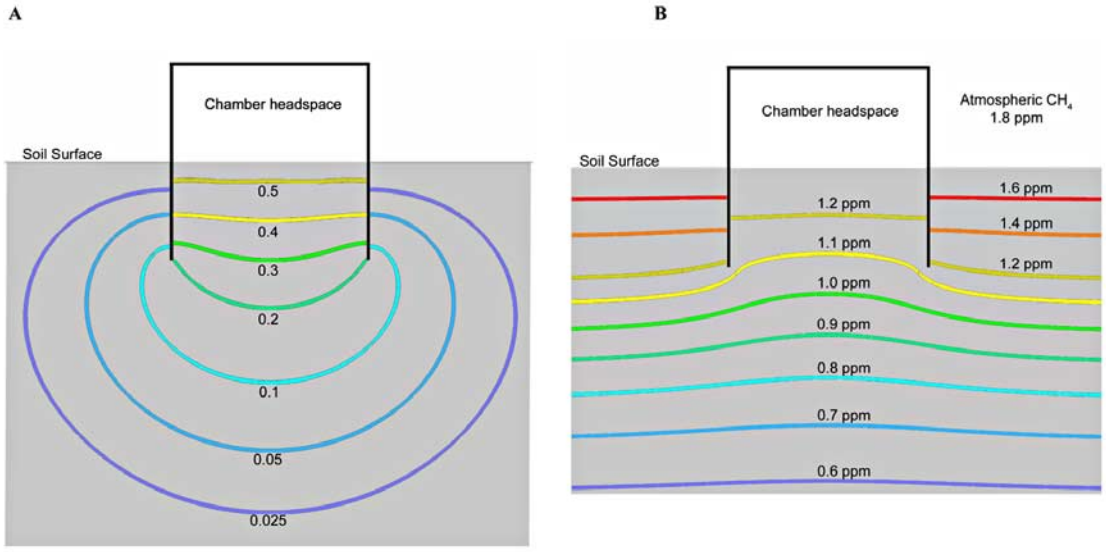

Figure 2. Vertical cross section of inserted chamber and base, with numerical simulation illustrating multidimensional flow of (a) a tracer gas (D = 1.97 cm^2 min^{-1}) and (b) methane (D = 2.96 cm^2 min^{-1}, μ = 0.01 min^{-1}). The 20 cm diameter cylindrical chamber is inserted 10 cm into a dry soil (θ = 0.046) of moderately high air-filled porosity (a = 0.41). The concentration isolines are shown at 40 min after insertion of the chamber and introduction of the tracer gas (at C_o = 1 unit concentration) and methane (at C_o = 1.8 ppm).

approaches zero. We selected a range of methanotroph activities (1×10^{-5} to 1×10^{-1} min^{-1}) to correspond to the range of observed methane flux rates, given the physical constraints imposed by diffusion. According to equation (12), very high methane flux rates (>5 mg CH_4-C m^{-2} d^{-1}) are only possible at the highest diffusivities and when methanotroph activity is ~0.1 min^{-1}. Flux rates below 0.01 mg CH_4-C m^{-2} d^{-1}, occurring at intermediate diffusivity values and very small methanotroph activities around 1×10^{-5} min^{-1}, are nearly undetectable using chamber methods. Visual inspection of Figure 1 and equation (12) reveals that doubling diffusivity or methanotroph activity leads to only $\sqrt{2}$ increase in flux rates.

4.2. Examination of Assumptions

4.2.1. One-Dimensional Flow Assumption

[30] Because our model assumes that all gas movement is along the vertical axis, lateral gas flow could lead to substantial errors in the estimation of D and μ. Failure to insert the chamber deep enough into the soil can allow tracer gas migration beyond the bounded soil during the measurement time, leading to an accelerated drop in the headspace concentration (relative to the one-dimensional case) and overestimation of D. Estimates of methanotroph activity would also be affected by multidimensional flow, both indirectly through error propagation of the poorly estimated D and through lateral diffusion of methane into the chamber from the surrounding soil. For the estimation of D from the tracer gas, *Rolston et al.* [1991] recommended insertion depths of 20 cm and measurement times of less than 50 min for dry soils. In hard, dry soils, chamber insertion to 20 cm depth may be impractical without excessive disturbance, and the enhanced gas diffusion introduced by cracking the soil in such cases may be more deleterious to measurement accuracy than the multidimensional flow effects.

[31] To assess errors from multidimensional effects in dry, highly porous soil with shallow chamber insertion in the estimation of D and μ, we used HYDRUS, a reaction-transport simulation software package [*Simunek et al.*, 2006], to simulate flow of both the tracer gas and methane by solving the flow equations using a finite element grid. Comparison of a 1-D simulation of methane dynamics in HYDRUS yielded identical results to those predicted by the analytical solution (equation (9)), thus confirming the accuracies of these two approaches.

[32] In Figure 2, we illustrate the simulated gas concentration profiles for a hypothetical soil and demonstrates the multidimensional effects. The lateral exit of the tracer gas (Figure 2a) through the lower reaches of the inserted chamber causes the headspace concentration to decrease more rapidly than if the flow had remained one-dimensional, and causes overestimation of D. The lateral concentration gradients for methane diffusion into the chamber are not as sharp (Figure 2b) but, in conjunction with the estimation error in D, these effects cause underestimation of μ.

[33] To quantify the magnitude of error in D and μ estimation caused by multidimensional flow and to suggest guidelines for insertion depths to minimize these errors, we repeated numerical simulations using HYDRUS for a wide range of D and μ values for a chamber inserted to various depths and measured over 30 min. We then analyzed the headspace tracer and methane concentrations versus time from these simulations to estimate the apparent D and μ for each run and compared these recovered parameters to the actual values used in the simulation. For example, in the numerical experiment illustrated in Figure 2a, analysis of the headspace concentration yields an apparent D that is 1.12 times larger than the actual D. The results of this error

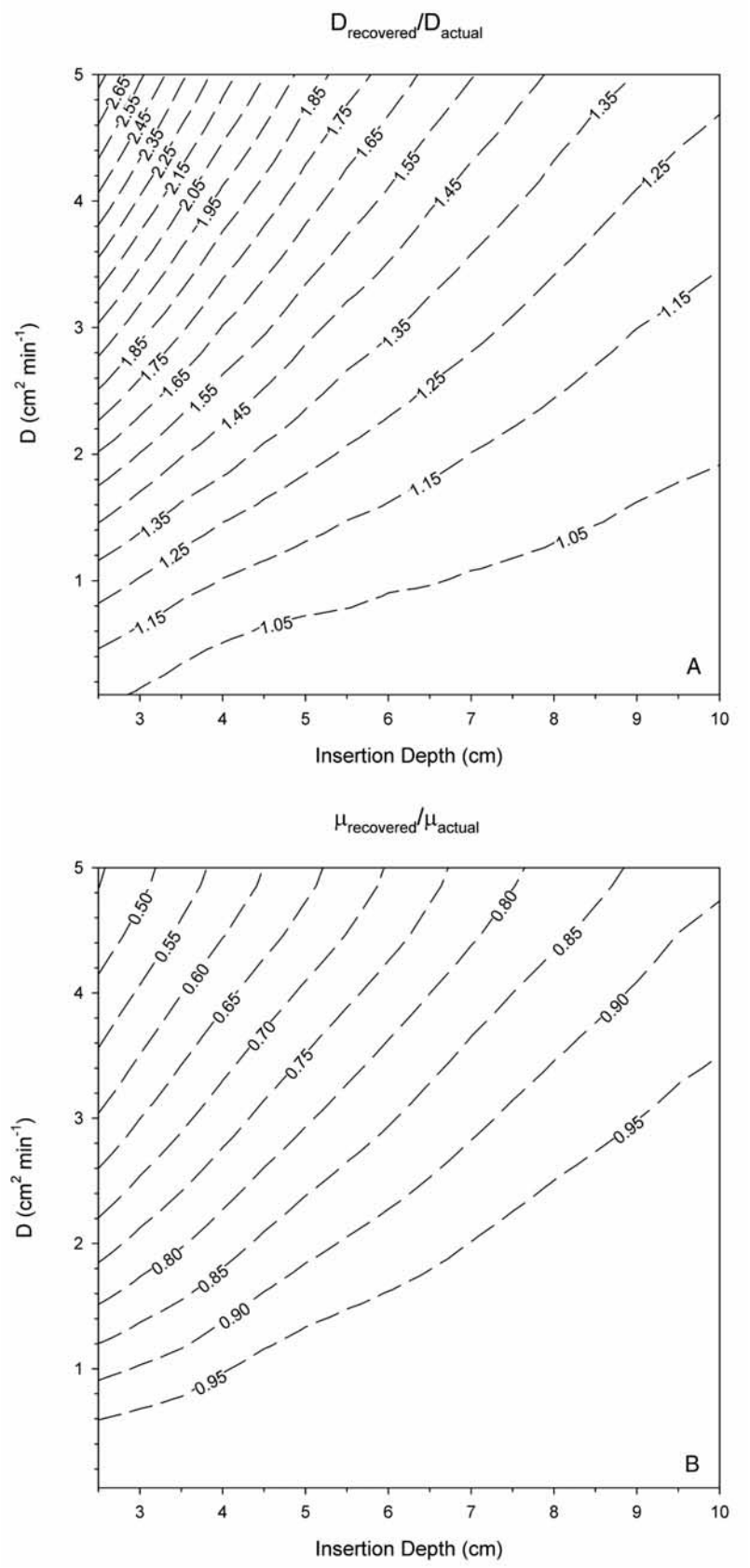
$D_{recovered}/D_{actual}$
D (cm^2 min^{-1})
Insertion Depth (cm)
A
$\mu_{recovered}/\mu_{actual}$
D (cm^2 min^{-1})
Insertion Depth (cm)
B

Figure 3

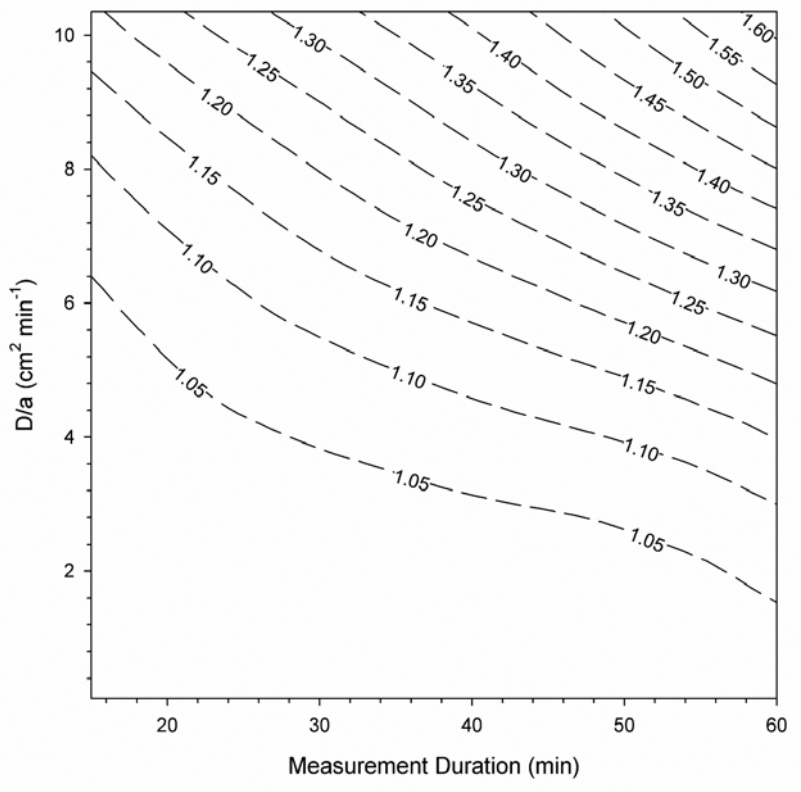

Figure 4. Effect of measurement duration on the recovery of D for a wide range of diffusion conditions. Results shown are for a 10 cm inserted chamber with a 10 cm high cylindrical, well-mixed headspace. The binary diffusion coefficient for the tracer gas in air is 8 cm^2 min^{-1}.

analysis for D (Figure 3a) and μ (Figure 3b) clearly reveal the danger of shallow chamber insertion in soil with high diffusivity. For the simulations, we selected a water content ($\theta = 0.05$) and air filled porosity ($a = 0.55$) that are typical of summertime grassland soils in the western United States, but may be a worst case for many researchers. For high D values of 3 cm^2 min^{-1}, estimation errors from a 10 cm insertion depth are about +15% for D and about −5% for μ. Naturally, the estimate errors worsen for longer measurement times.

[34] To provide guidelines for choosing appropriate flux chamber deployment times, we illustrate (Figure 4) the effect of measurement duration on the recovery of D for a wide range of soil conditions with a 10 cm inserted chamber. When planning field deployments of chambers, the D is not known a priori, but it could be estimated from the product of the free-air diffusion coefficient of the tracer gas (D_{air}) and a soil tortuosity factor such as $\xi = a^{(10/3)}/\varphi^2$, where φ is the total soil porosity [*Millington and Quirk*, 1961]. Using such an approach for very dry conditions and a tracer gas with D_{air} = 8 cm^2 min^{-1}, the expected D/a is about 6 cm^2 min^{-1} and, from Figure 3a, a 20 min measurement would be expected to overestimate the actual soil D by about 5%. This error from multidimensional flow might be considered tolerable whereas a 50 min measurement with the roughly 20% overestimation is rejected. For less extreme conditions ($a < 0.4$), $D/a < 4$ cm^2 min^{-1} should be expected and measurement durations of 30 min or less would typically have errors of less than 5%. In general, we conclude that even in very dry soils where tracer D values as high as 3 cm^2 min^{-1} might be found, insertion depths near 10 cm for a 15–30 min. measurement period appear reasonable for applying a one-dimensional analysis to the headspace concentration data.

4.2.2. Vertical Homogeneity Assumption

[35] Vertical homogeneity is a mathematical convenience that is rarely found in nature; factors affecting gas flow such as soil water content and soil porosity typically vary with depth. To give a sense of the magnitude of the errors, we used HYDRUS simulations to examine the effect of vertical heterogeneity on the estimation of D and μ for two hypothetical soils.

[36] We examine two scenarios with strong, plausible changes in properties near the soil surface. To highlight biological heterogeneity, we considered a soil with uniform porosity ($\varphi = 0.47$), water content ($\theta = 0.20$) and diffusivity

Figure 3. Effect of three-dimensional flow on recovery of the diffusion coefficient from a 30 min duration measurement. Results shown are from numerical simulation of a dry, high-porosity soil ($\theta = 0.05$, $a = 0.55$) with a range of chamber insertion depths and a 10 cm high cylindrical, well-mixed headspace. (a) The free-air diffusion coefficient for the tracer gas in air (D_{air}) is 8 cm^2 min^{-1}. (b) The free-air diffusion coefficient (D_{air}) for methane is 12 cm^2 min^{-1}, and the degradation coefficient is $\mu = 0.01$ min^{-1}.

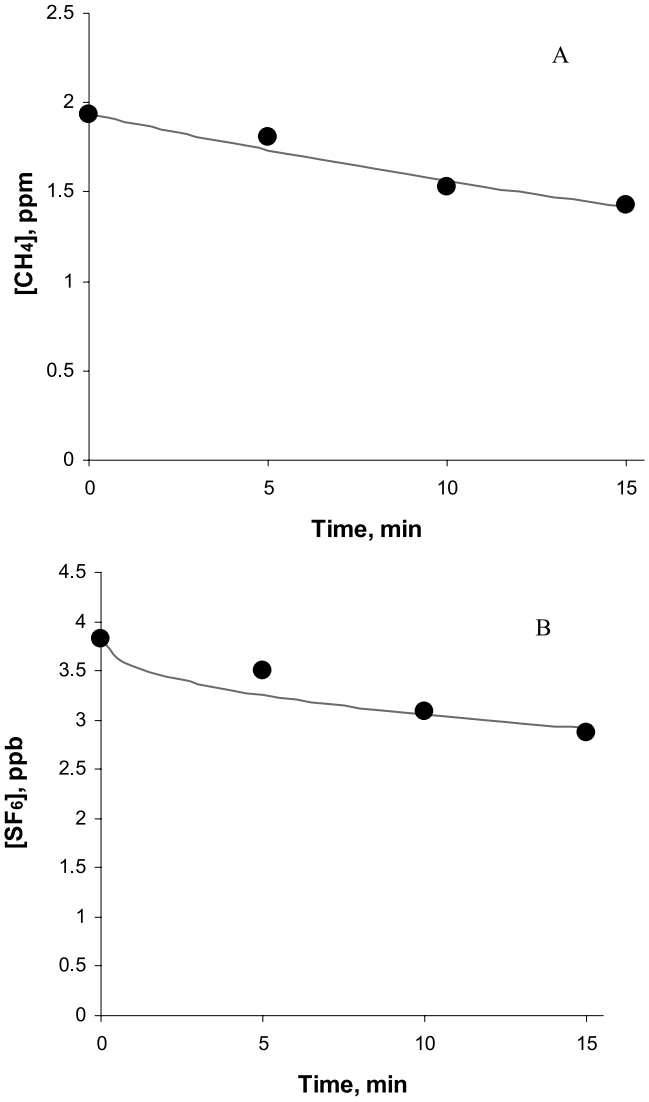

Figure 5. Example of model fit (lines) to field data (points) for (a) the inert tracer gas SF_6 and (b) the reactive gas methane (CH_4). Data are for a chamber height (H) 9.1 cm with air-filled porosity (a) 0.39. Concentrations of the inert tracer gas at 0, 5, 10, and 15 min are 3.821, 3.501, 3.092, and 2.870 ppb while methane concentrations are 1.935, 1.803, 1.528, and 1.428 ppm. Fitting equation (3) to the inert tracer gas data yields a diffusivity (D) for SF_6 (molecular weight 146) of 0.95 cm^2 min^{-1}, corresponding to a CH_4 diffusivity (molecular weight 16) of 1.44 cm^2 min^{-1}. Best fit of the methane data to equation (10) occurs with a methanotroph activity (μ) of 0.083 min^{-1}. The r^2 values for model fits to data are 0.91 for SF_6 and 0.97 for CH_4. Although the methane flux rate calculated from linear regression of the concentration change yields an estimated 2.33 mg CH_4-C m^{-2} d^{-1}, application of equation (12) indicates that the flux rate in the absence of the chamber (i.e., under field conditions) is 22% higher: 2.99 mg CH_4-C m^{-2} d^{-1}.

($D = 0.7$ cm^2 min^{-1}), but with a profile of the methanotroph activity, such that μ decreased by an order of magnitude from 0.02 to 0.002 min^{-1} between the soil surface and 10 cm depth. Using HYDRUS to simulate a 30 min experiment with chamber inserted 10 cm, application of the analytical approach (section 3.2.3) to the simulated concentration data in the headspace returns $\mu = 0.009$ min^{-1}. The actual methane flux into this soil is 0.73 mg CH_4 m^{-2} d^{-1}, while our estimated flux using $\mu = 0.009$ min^{-1} and $D = 0.7$ cm^2 min^{-1} in equation (12) would be 0.70 mg CH_4 m^{-2} d^{-1}. Hence, heterogeneity in μ as describe here would return an intermediate value for μ, and would result in about 4% higher estimate of flux.

[37] To illustrate a possible effect of physical heterogeneity, we considered a soil with uniform $\mu = 0.01$ min^{-1} and uniform porosity (0.47), but with water content increasing linearly from 0.02 at the soil surface to 0.2 at 10 cm depth and beyond. The HYDRUS model D value, which is derived from the Millington-Quirk relationship, decreases from 3.8 to 0.7 cm^2 min^{-1} in the upper 10 cm of this hypothetical soil. Analysis of the simulated tracer and methane concentrations returns an intermediate diffusivity (2.21 cm^2 min^{-1}) and ~50% lower value for μ (0.0047 min^{-1}). The actual methane flux in this case is 1.1 mg CH_4 m^{-2} d^{-1}, while we would estimate the flux using the returned D and μ at 0.92 mg CH_4 m^{-2} d^{-1}, a 16% underestimate.

4.3. Field Measurements

[38] In application of the chamber method to the grassland soils, we found good agreement between trends in chamber gas concentrations and equations (3) and (10) (Figure 5). Consistent with model predictions, we regularly observed a nearly linear decline in methane concentration, and a characteristically nonlinear decline in the inert tracer gas concentrations. The fit of SF_6 data to equation (3) gave r^2 values >0.89 in more than 50% of cases, and >0.75 in 75% of cases. Similarly, the fit of CH_4 data to equation (10) gave r^2 values >0.89 in >50% of cases, and >0.70 in 75% of cases. The lowest 25% of r^2 values were primarily associated with conditions of low rates of diffusion or CH_4 uptake. In these cases, the observed variance in concentration was primarily from analytical noise.

[39] Field data of all soil properties showed coherent temporal patterns (Figure 6). Over a relatively dry period between May 2 and June 20, soil moisture declined by half from 38% to 15% while soil temperatures warmed from 14 to 28°C (data not shown). Coincidently, soil diffusivity doubled from about 1.1 to >2.6 cm^2 min^{-1}. While this increase in diffusivity might have allowed greater rates of methane uptake, we instead observed that methane uptake fell by 40% during this interval. Application of our approach revealed that methanotroph activity (μ) fell by >90% from 0.036 min^{-1} to 0.0033 min^{-1}. Over this same time period, soil respiration rates also fell from 7.8 to 1.4 g CO_2-C m^{-2} d^{-1} (data not shown). Following a rain event on July 5, diffusivity fell, but soil moisture, methanotroph activity, soil respiration and methane uptake rates all rose. In Figure 7 we illustrate that 88% of the observed variation in methanotroph activity can be explained by changes in soil moisture.

5. Discussion

5.1. Analysis of Approach

[40] Over a wide range of environmental conditions and flux rates, our model closely fit measured changes in

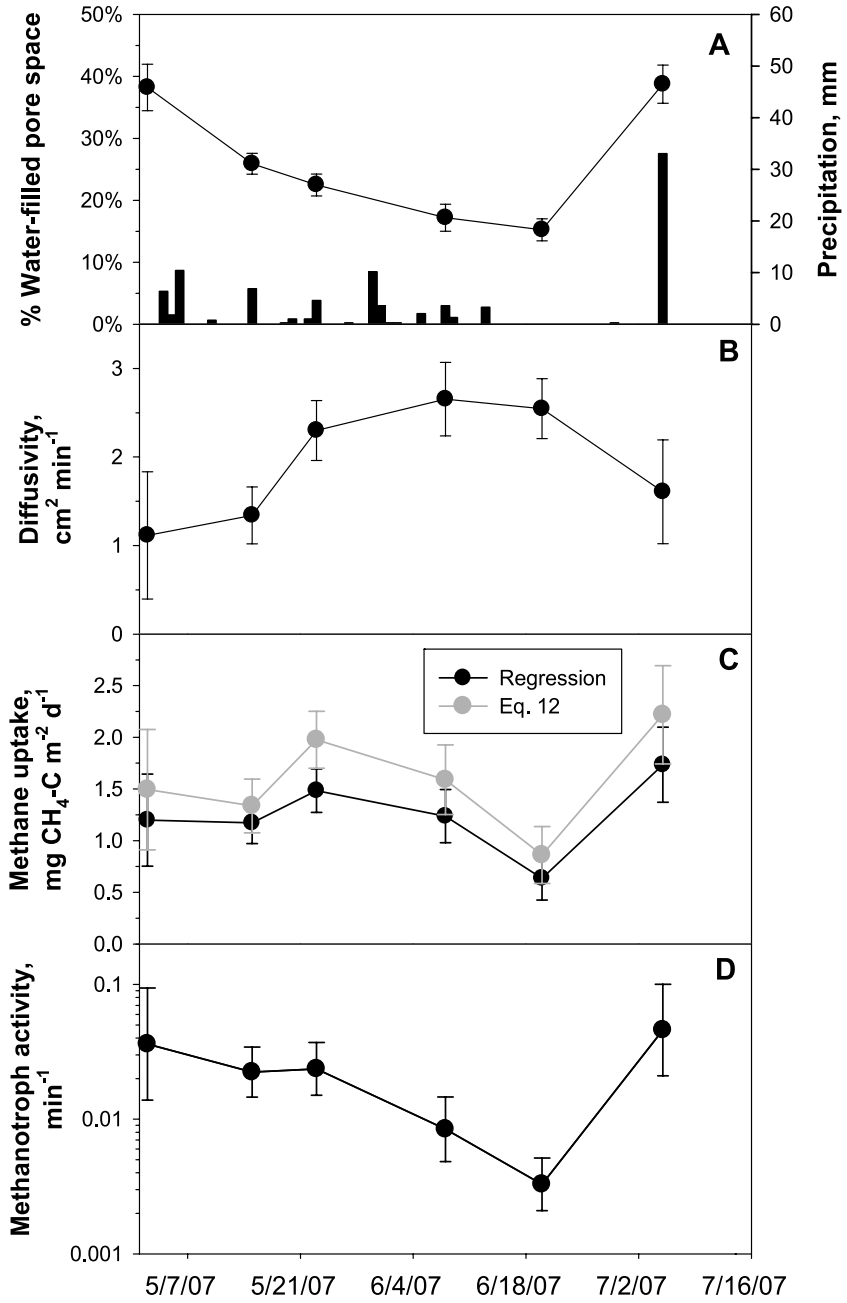

Figure 6. Application of approach to soils on the Shortgrass Steppe Long-Term Ecological Research (SGS LTER) from 2 May to 5 July 2007. (a) Soil moisture (points) and precipitation events (bars), (b) soil diffusivity, (c) methane uptake rate, and (d) methanotroph activity (note the log scale). Figure 6c shows results from two calculations of methane flux rates: by typical linear regression of methane concentration over time (''regression'') and when excluding chamber effects (equation (12)). Error bars are 1 SE; methanotroph activity results were lognormally distributed, so the mean and error were determined from log-transformed data.

methane concentrations, indicating that we have accurately characterized the biophysical processes underlying methane uptake. We anticipate that greater temporal resolution of concentration trends will allow future models to include more sophisticated treatment of the depth distributions of soil diffusivity and methanotroph activity.

[41] Some authors have suggested that variability in methanotroph activity is only important in the absence of ''diffusive limitation'' to methane uptake [*Ball et al.*, 1997; *Reay et al.*, 2001]). While this notion parallels the ecological view of single-nutrient limitation in ecosystems, our analytic solution (equation (12)) clearly shows that diffusivity and methanotroph activity always ''colimit'' the rate of methane consumption by upland soils at all magnitudes of these parameters; no matter what the diffusivity, doubling the methanotroph activity will always lead to $\sqrt{2}$ increase in

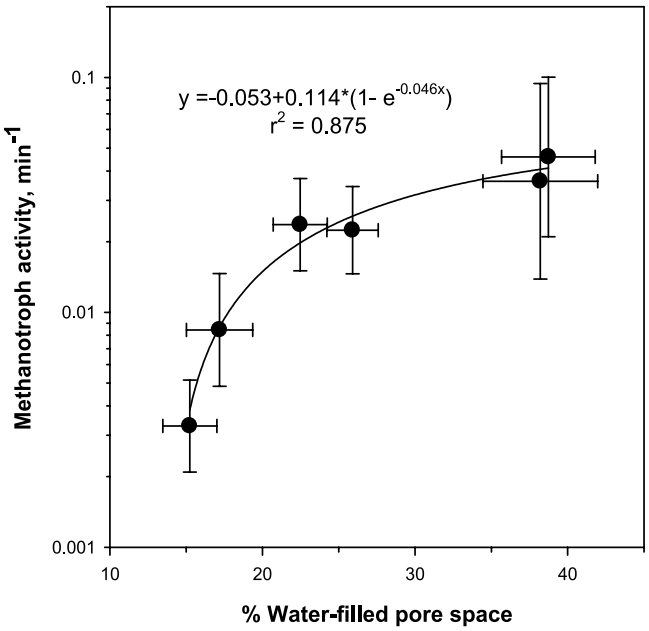

Figure 7. Relationship between methanotroph activity (μ) and soil moisture as percent of soil pores filled with water from the data shown in Figure 6. Error bars are 1 SE.

methane consumption rate. The square root relationship in equation (12) further predicts that methane uptake rates will be nonlinearly related to environmental factors that influence methanotroph activity, including temperature, moisture and levels of inhibitory compounds.

[42] Comparisons of the analytical solution and HYDRUS simulations, beyond characterizing lateral gas transport, also illustrated two important effects of vertical heterogeneity on the estimates of diffusivity and methanotroph activity. First, we found reassuring evidence that field application of our technique returned intermediate diffusivity values for soils with nonuniform diffusivity, and intermediate methanotroph activities for soils with nonuniform activity. Second, we found that field estimates of methanotroph activity depend on sufficient soil diffusivity to communicate the biological activity to the chamber. Reduced diffusive connection between surface and deeper soils causes poor communication and a reduced estimate of activity. Thus, differences in methanotroph activity among soils may need to be interpreted in light of both biological differences and possible soil diffusivity profiles. Such scenarios may be rare in nature, however, because high rates of methanotroph activity are not likely to persist in regions of soil with low diffusivity; weak diffusive connection with the atmosphere would starve the methanotrophs. To better evaluate these effects, future work should use physiologically based models to investigate the potential for vertical distributions of methanotroph activity to follow vertical distributions in diffusivity.

[43] An additional application of our approach would be to study the kinetic isotopic effects (i.e., ratios of $^{13}C/^{12}C$ and D/H) of methane uptake using static flux chambers. [*Snover and Quay*, 2000] conducted such an investigation, but their approach required measurement of the soil methane concentration gradients, and it did not directly measure soil diffusivity. These differences are largely a matter of convenience, but our HYDRUS simulations raise questions about other artifacts of their study. Their field deployments lasted an average of 8 h and induced ~40% depletion in methane concentrations, but they used chamber bases inserted only 8–10 cm into the soil. Our HYDRUS simulations suggest that 2-D effects likely caused underestimates of methanotroph activity, with cascading errors in the kinetic isotope effects as a result. In cases where such long deployment times are unavoidable, future studies should employ a 2-D simulation model to correct for lateral gas movement.

5.2. Ecology of Methanotrophic Bacteria

[44] Our field results highlight the value of directly measuring the individual mechanisms that collectively drive differences in methane uptake rates. Previous studies have shown reduced methane uptake rates at lower soil moisture levels [*Gulledge and Schimel*, 1998b], but the way in which this water limitation is expressed under field conditions has remained obscured by the confounding effects of changing soil gas diffusivity. Laboratory experiments with sieved soils can expose some facets of this water limitation [e.g., Reay et al. 2001], but with limited inference, since the soil structure is destroyed in the process [*Madsen*, 1998].

[45] Our observation of reduced methane uptake under drought conditions can be used to consider potential tradeoffs among the microhabitats inhabited by methanotrophs. As soils dry, water is lost progressively from the largest pores to the smallest pores, and so the smaller pores retain water longer during dry periods. However, the diffusive supply of methane is slower through the more tortuous small pores as compared to larger pores. Thus, methanotrophs experience a tradeoff between optimal conditions for methane supply versus water. If most methanotrophs live along large pores, methanotroph activity should show steep declines in activity with falling soil moisture levels. In contrast, if methanotrophs live along smaller pores deeper in the soil matrix, methanotroph activity should be maintained until very low soil moisture levels.

[46] The steep declines that we observed in methanotroph activity with falling soil moisture (Figure 7) are consistent with methanotrophs living preferentially in larger pore spaces. This microhabitat preference is also consistent with methanotroph physiology studies showing that methanotroph growth rates are very slow and strongly methane-limited at subatmospheric methane concentrations [*Conrad*, 1999]. The fact that soils of the Shortgrass Steppe undergo frequent summer droughts suggests that methanotrophs there must be uniquely adapted to tolerate desiccation cycles. Future evaluation of this hypothesis can come from comparing the water response curves of methanotrophs from sites of differing drought stress.

[47] We anticipate that future applications of this approach, especially when applied in conjunction with molecular tools for determining methanotroph distribution and abundance, have the potential to more clearly reveal the factors that determine the ecology of methanotrophs in their natural setting. Such measures have tremendous potential for building the "genes to ecosystems" bridge that has proven difficult for many other biogeochemical processes.

[48] **Acknowledgments.** This research was supported by NSF DEB 0445302 to JvF and by NSF DEB 0217631 to the Shortgrass Steppe Long-Term Ecological Research project. Anita Kear contributed invaluable efforts in the field and laboratory, and Caroline Yonker assisted with field site selection.

References

Ball, B. C., K. A. Smith, L. Klemedtsson, R. Brumme, B. K. Sitaula, S. Hansen, A. Prieme, J. MacDonald, and G. W. Horgan (1997), The influence of soil gas transport properties on methane oxidation in a selection of northern European soils, *J. Geophys. Res.*, *102*(D19), 23,309–23,317, doi:10.1029/97JD01663.

Bender, M., and R. Conrad (1992), Kinetics of CH_4 oxidation in oxic soils exposed to ambient air or high CH_4 mixing ratios, *FEMS Microbiol. Ecol.*, *101*, 261–270.

Carslaw, H. S., and J. C. Jaeger (1959), *Conduction of Heat in Solids*, 2nd ed., 510 pp., Clarendon Press, Oxford.

Conrad, R. (1999), Soil microorganisms oxidizing atmospheric trace gases, *Indian J. Microbiol.*, *39*, 193–203.

Dunfield, P., and R. Conrad (2000), Starvation alters the apparent half-saturation constant for methane in the type II methanotroph methylocystis strain LR1, *Appl. Environ. Microbiol.*, *66*(9), 4136–4138, doi:10.1128/AEM.66.9.4136-4138.

Epstein, H. E., I. C. Burke, A. R. Mosier, and G. L. Hutchinson (1998), Plant functional type effects on trace gas fluxes in the shortgrass steppe, *Biogeochemistry*, *42*(1–2), 145–168, doi:10.1023/A:1005959001235.

Fenchel, T., G. M. King, and T. H. Blackburn (1998), *Bacterial Biogeochemistry: The Ecophysiology of Mineral Cycling*, 307 pp., Academic, San Diego, Calif.

Green, J. L., B. J. M. Bohannan, and R. J. Whitaker (2008), Microbial biogeography: From taxonomy to traits, *Science*, *320*(5879), 1039–1043, doi:10.1126/science.1153475.

Gulledge, J., and J. Schimel (1998a), Low-concentration kinetics of atmospheric CH_4 oxidation in soil and mechanism of NH_4^+ inhibition, *Appl. Environ. Microbiol.*, *64*(11), 4291–4298.

Gulledge, J., and J. P. Schimel (1998b), Moisture control over atmospheric methane consumption and CO_2 production in diverse Alaskan soils, *Soil Biol. Biochem.*, *30*(8–9), 1127–1132, doi:10.1016/S0038-0717(97)00209-5.

Healy, R., R. Striegl, T. Russell, G. Hutchinson, and G. Livingston (1996), Numerical evaluation of static-chamber measurements of soil–atmosphere gas exchange: Identification of physical processes, *Soil Sci. Soc. Am. J.*, *60*(3), 740–747.

Hillel, D. (1982), *Introduction to Soil Physics*, 365 pp., Academic, San Diego, Calif.

Horz, H. P., V. Rich, S. Avrahami, and B. J. M. Bohannan (2005), Methane-oxidizing bacteria in a California upland grassland soil: Diversity and response to simulated global change, *Appl. Environ. Microbiol.*, *71*(5), 2642–2652, doi:10.1128/AEM.71.5.2642-2652.2005.

Jost, W. (1960), *Diffusion in Solids, Liquids and Gases*, 558 pp., Academic, San Diego, Calif.

Jury, W. A., and R. Horton (2004), *Soil Physics*, 370 pp., John Wiley, Hoboken, N. J.

King, G. M. (1997), Responses of atmospheric methane consumption by soils to global climate change, *Global Change Biol.*, *3*, 351–362, doi:10.1046/j.1365-2486.1997.00090.x.

Knief, C., A. Lipski, and P. Dunfield (2003), Diversity and activity of methanotrophic bacteria in different upland soils, *Appl. Environ. Microbiol.*, *69*(11), 6703–6714, doi:10.1128/AEM.69.11.6703-6714.2003.

Livingston, G. P., and G. L. Hutchinson (1995), Enclosure-based measurement of trace gas exchange: Applications and sources of error, in *Biogenic Trace Gases: Measuring Emissions From Soil and Water*, edited by P. A. Matson and R. C. Hariss, 394 pp., Blackwell Sci. Ltd., Cambridge, UK.

Madsen, E. L. (1998), Epistemology of environmental microbiology, *Environ. Sci. Technol.*, *32*, 429–439, doi:10.1021/es970551y.

Millington, R. J., and J. P. Quirk (1961), Permeability of porous solids, *Trans. Faraday Soc.*, *57*, 1200–1207, doi:10.1039/tf9615701200.

Mosier, A. R., L. K. Klemedtsson, R. A. Sommerfeld, and R. C. Musselman (1993), Methane and nitrous oxide flux in a Wyoming subalpine meadow, *Global Biogeochem. Cycles*, *7*(4), 771–784, doi:10.1029/93GB02561.

Mosier, A. R., W. J. Parton, D. W. Valentine, D. S. Ojima, D. S. Schimel, and J. A. Delgado (1996), CH_4 and N_2O fluxes in the Colorado shortgrass steppe: 1. Impact of landscape and nitrogen addition, *Global Biogeochem. Cycles*, *10*(3), 387–399, doi:10.1029/96GB01454.

Mosier, A., W. Parton, D. Valentine, D. Ojima, D. Schimel, and O. Heinemeyer (1997), CH_4 and N_2O fluxes in the Colorado shortgrass steppe: 2. Long-term impact of land use change, *Global Biogeochem. Cycles*, *11*(1), 29–42, doi:10.1029/96GB03612.

Mosier, A., W. Parton, and S. Phongpan (1998), Long-term large N and immediate small N addition effects on trace gas fluxes in the Colorado shortgrass steppe, *Biol. Fertil. Soils*, *28*(1), 44–50, doi:10.1007/s003740050461.

Mosier, A. R., J. A. Morgan, J. Y. King, D. LeCain, and D. G. Milchunas (2002), Soil-atmosphere exchange of CH_4, CO_2, NO_x, and N_2O in the Colorado shortgrass steppe under elevated CO_2, *Plant Soil*, *240*(2), 201–211, doi:10.1023/A:1015783801324.

Radajewski, S., G. Webstera, D. Reayb, S. Morris, P. Ineson, D. Nedwell, J. Prosser, and J. Murrell (2002), Identification of active methylotroph populations in an acidic forest soil by stable-isotope probing, *Microbiology*, *148*(8), 2331–2342.

Reay, D. S., D. B. Nedwell, and N. McNamara (2001), Physical determinants of methane oxidation capacity in a temperate soil, *Water Air Soil Pollut. Focus*, *1*(5), 401–414, doi:10.1023/A:1013121010356.

Rolston, D. E., R. D. Glauz, G. L. Grundmann, and D. T. Louie (1991), Evaluation of an in situ method for measurement of gas diffusivity in surface soils, *Soil Sci. Soc. Am. J.*, *55*, 1536–1542.

Roslev, P., N. Iversen, and K. Henriksen (1997), Oxidation and assimilation of atmospheric methane by soil methane oxidizers, *Appl. Environ. Microbiol.*, *63*(3), 874–880.

Schimel, J. P. (2001), Biogeochemical cycles: Implicit vs. explicit microbiology, in *Global Biogeochemical Cycles in the Climate System*, edited by E. D. Schultze et al., pp. 177–183, Academic, San Diego, Calif.

Simunek, J., D. Jacques, M. T. van Genuchten, and D. Mallants (2006), Multicomponent geochemical transport modeling using Hydrus-1D and HP1, *J. Am. Water Resour. Assoc.*, *42*(6), 1537–1547, doi:10.1111/j.1752-1688.2006.tb06019.x.

Smith, K. A., T. Ball, F. Conen, K. E. Dobbie, J. Massheder, and A. Rey (2003), Exchange of greenhouse gases between soil and atmosphere: Interactions of soil physical factors and biological processes, *Eur. J. Soil Sci.*, *54*(4), 779–791, doi:10.1046/j.1351-0754.2003.0567.x.

Snover, A. K., and P. D. Quay (2000), Hydrogen and carbon kinetic isotope effects during soil uptake of atmospheric methane, *Global Biogeochem. Cycles*, *14*(1), 25–39, doi:10.1029/1999GB900089.

von Fischer, J. C., and L. O. Hedin (2002), Separating methane production and consumption with a field-based isotope pool dilution technique, *Global Biogeochem. Cycles*, *16*(3), 1034, doi:10.1029/2001GB001448.

G. Butters, Department of Soil and Crop Sciences, Colorado State University, Fort Collins, CO 80523, USA.

P. C. Duchateau, Department of Mathematics, Colorado State University, Fort Collins, CO 80523, USA.

R. Siller, Department of Biology, University of Michigan, Ann Arbor, MI 48109, USA.

R. J. Thelwell, Department of Mathematics and Statistics, James Madison University, Harrisonburg, VA 22807, USA.

J. C. von Fischer, Department of Biology, Colorado State University, Fort Collins, CO 80523, USA. (jcvf@colostate.edu)